Communication

Previous Article | Next Article | Articles ASAP

Minimal Heterochiral *de Novo* Designed 4Fe–4S Binding Peptide Capable of Robust Electron Transfer

J. Dongun Kim[†¶+], Douglas H. Pike[‡¶], Alexei M. Tyryshkin[†], G. V. T. Swapna[‡§], Hagai Raanan[†], Gaetano T. Montelione[‡§∥], Vikas Nanda[*‡∥], and Paul G. Falkowski[*†⊥]

[†] Environmental Biophysics and Molecular Ecology Program, Department of Marine and Coastal Sciences, Rutgers, the State University of New Jersey, New Brunswick, New Jersey 08901, United States
[‡] Center for Advanced Biotechnology and Medicine, Rutgers, the State University of New Jersey, Piscataway, New Jersey 08854, United States
[§] Department of Molecular Biology and Biochemistry, Rutgers, the State University of New Jersey, Piscataway, New Jersey 08854, United States
[∥] Department of Biochemistry and Molecular Biology, Robert Wood Johnson Medical School, Rutgers, the State University of New Jersey, Piscataway, New Jersey 08854, United States
[⊥] Department of Earth and Planetary Sciences, Rutgers, the State University of New Jersey, Piscataway, New Jersey 08854, United States

J. Am. Chem. Soc., Article ASAP
DOI: 10.1021/jacs.8b07553
Publication Date (Web): August 24, 2018

*nandavi@cabm.rutgers.edu, *falko@marine.rutgers.edu

Cite this: *J. Am. Chem. Soc.* XXXX, XXX, XXX-XXX
RIS Citation GO

Article Options

ACS ActiveView PDF
Hi-Res Print, Annotate, Reference QuickView
PDF *(1101 KB)*
PDF w/ Links *(341 KB)*
Full Text HTML

Abstract
Supporting Info
Figures
References

Add to Favorites
Download Citation
Email a Colleague
Order Reprints
Rights & Permissions
Citation Alerts

Add to ACS ChemWorx

SciFinder A CAS SOLUTION Sign in

Retrieve Detailed Record of this Article
Retrieve Substances Indexed for this Article
Retrieve All References Cited for this Article

Explore by:
Author of this Article
Any Author
Research Topic

Kim, J. Dongun | Search

Metrics

Abstract

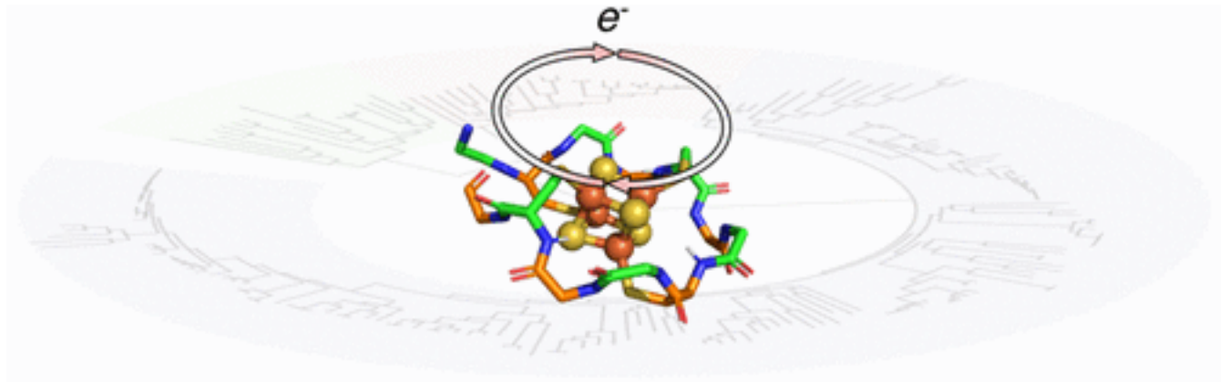

Ambidoxin is a designed, minimal dodecapeptide consisting of alternating L and D amino acids that binds a 4Fe–4S cluster through ligand–metal interactions and an extensive network of second-shell hydrogen bonds. The peptide can withstand hundreds of oxidation–reduction cycles at room temperature. Ambidoxin suggests how simple, prebiotic peptides may have achieved robust redox catalysis on the early Earth.

The 4Fe–4S cubane cluster is a ubiquitous inorganic cofactor mediating a wide variety of electron transfer reactions across the tree of life.(1) The structurally conserved ferredoxin fold binds a 4Fe–4S cubane cluster with four cysteine residues in a common sequence motif (Cys-X_1-X_2-Cys-X_3-

X_4-Cys-$(X)_n$-Cys).(2–4) The ferredoxin α/β topology is one of a small number of folds proposed to have given rise to myriad proteins.(5) The origin and evolution of the ferredoxin fold family was likely a key evolutionary milestone in origins of biological electron transfer.(6) Although the structures of ferredoxins are well studied, it has proven challenging to design simpler, artificial peptides that stably bind iron–sulfur complexes and are capable of reversible electron transfer reactions. *De novo* designs based on intrinsic symmetry of iron–sulfur clusters have produced artificial folds that bind metal and exhibit reversible redox stability for a few dozen cycles.(7–9) Here, we present a minimal dodecapeptide ferredoxin, consisting of alternating L and D amino acid residues, comprised only of cysteine with arginine or lysine. This peptide binds an 4Fe–4S cluster through ligand–metal interactions and an extensive network of second-shell hydrogen bonds. The resulting "ambidoxin" peptide has robust redox stability; the holo-peptide can undergo hundreds of oxidation–reduction cycles at room temperature.

Analyses of backbone dihedral angles of iron–sulfur cluster binding heptapeptide (CXXCXXC) fragments from nonredundant structures in the Protein Data Bank (Figure 1a,b) revealed a five-residue alternating alpha-left and alpha-right structural motif. This motif is similar to the alpha-pleated sheet postulated by Pauling,(10) and nest motifs observed by Watson and Milner-White.(11,12) Extending this pattern to 12 residues produces a unique curved backbone that encircles the iron sulfur cluster (Figure 1c,d, S1). This unusual conformation could be enforced with a sequence of alternating L and D amino acids that stabilize alpha-right and alpha-left backbone conformations respectively (Figure S1g). Molecular dynamics simulations, starting from geometrically and energetically idealized conformations, converged on a unique stable structure that closely aligns with natural ferredoxin (Figure 1e, S1). Because of the equal contributions of L and D amino acids in the design, we refer to this class of molecules as "ambidoxins".

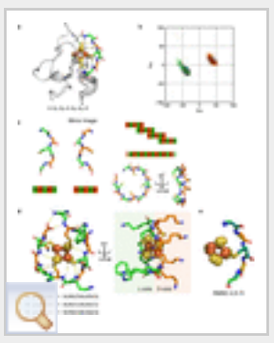

Figure 1. Design of ambidoxin. (a) Bacterial ferredoxin has a conserved CXXCXXC motif near iron sulfur cluster structures. (b) Ramachandran plot of the X_1-X_2-C-X_3-X_4 sequence motif surrounding the central cysteine reveals conserved alpha-right conformation (R) in X_1 and X_4 positions (green) and alpha-left conformation (L) in X_2 an X_3 positions (orange). (c) Ferredoxin loop was built by extending the original XXCXX peptide ($\alpha_R\alpha_L\alpha_R\alpha_L\alpha_R$ conformation) with its mirror image ($\alpha_L\alpha_R\alpha_L\alpha_R\alpha_L$ conformation), maintaining an alternating right/left conformation throughout. (d) Sequences and computationally determined structural models of ambidoxin peptides. (e) Portion of ambidoxin model and natural ferredoxin structures are superimposable.

Given the stability of the 4Fe–4S cubane cluster in the absence of oxygen,(13,14) we expected that reconstitution of peptides in the presence of iron and sulfur salts would assemble as a cluster fully coordinated by a single peptide. To test this, we synthesized three ambidoxin variants that included either basic or acidic amino acids at the positions between cysteines, and a tryptophan at the third position to allow quantification by absorption at 280 nm. Upon iron–sulfur cluster assembly, **K** and **R** ambidoxin peptides showed a 420 nm charge-transfer absorption band prior to reduction with sodium dithionite (Figure S6),(15) and rhombic EPR signatures consistent with a bound 4Fe–4S cluster in the reduced state after treatment with sodium dithionite (Figure 2a, S8).(16–18) Holo-peptide yields of 80–94% were determined by spin counting experiments. Dipole–dipole interactions between clusters were not observed by EPR, supporting the presence of a monomeric holo-peptide. After reconstitution, holo-peptides were stable for days under anaerobic conditions at room temperature from pH 5 to 8 (Figure S9).

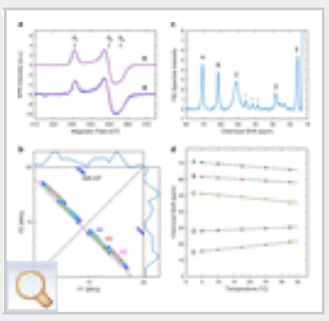

Figure 2. Structural characterization of ambidoxin. (a) X-band EPR spectra of a dithionite-reduced $[4Fe–4S]^+$ cluster reconstituted in **K** and **R** peptides in HEPES/pH 5.0 buffer, measured at 9.48 GHz and 10 K (blue traces). The simulated spectra (red dashed traces) used three rhombic g-factor values (g_1 = 2.0445, g_2 = 1.9365, g_3 = 1.903) as marked by vertical lines. (b) Cosine HYSCORE spectrum for $[4Fe–4S]^+$ cluster with **K** peptide in deuterated HEPES buffer at pH 5.0, measured at magnetic field 340 mT (cp. the g_1 field position in panel a) and temperature 12 K. Cross-peaks from three nonexchangeable cysteine protons (H1–H3) were resolved. (c) 600 MHz ^{1}H NMR spectrum of a dithionite-reduced $[4Fe–4S]^+$ cluster reconstituted in **K** peptide in 95% D_2O HEPES-d_{18}/pH 8.5 buffer measured at 278 K. Hyperfine shifted lines (labeled A–E) are from β-CH_2 protons of four cysteines ligating to paramagnetic $[4Fe–4S]^+$ cluster. Weak resonances marked with asterisks are from unknown minor (<10%) species. (d) Temperature dependence of the chemical shifts: Lines A–C with Curie temperature dependence are from four β-CH_2 protons of two cysteine ligands bound to mixed-valence $Fe^{2.5+}$–$Fe^{2.5+}$ pair, and lines D–E with anti-Curie dependence are from two β-CH_2 protons of two cysteine ligands bound to ferrous Fe^{2+}–Fe^{2+}

pair.

We did not observe cluster binding to the negatively charged **E** peptide (Figure S7). Assembled 4Fe–4S–4(Cys) complexes would have a –2 or –3 charge depending on the oxidation state. It is plausible that the significant charge associated with seven surrounding glutamates electrostatically destabilizes the holo-peptide, preventing assembly.

To validate the modeled structure of the paramagnetic peptide-cluster complex, we examined proton hyperfine interactions within 4 Å of the cluster by pulsed-EPR methods. Orientation-selective ESEEM and HYSCORE experiments were performed at several magnetic field positions across the rhombic EPR line-shape (Figures S10, S12–S17).(19,20) Both techniques consistently identified several protons strongly coupled to an unpaired electron spin residing on the 4Fe–4S cluster. Experiments in deuterated buffer revealed that four protons (labeled H1–H4 in Figure 2b, S16–S17) were nonexchangeable and likely belong to β-protons of the four cysteine ligands. From the HYSCORE cross-peak analysis (Figure S18), we were able to extract isotropic and anisotropic hyperfine coupling constants of the four protons, including relative orientations of their anisotropic hyperfine tensors with respect to the g_1 axis of electron g-factor (Table S2). These hyperfine parameters provided both Fe–H distances and angles between Fe–H vectors and the g_1 axis, providing eight constraints that were consistent with models from molecular mechanics simulations of ambidoxin (Figure S19 and Table S2).

To resolve the structure and electronic state of the cluster at ambient temperature, we performed paramagnetic NMR experiments(21) from 5 to 32 °C on holo-**K** peptide prepared to near-stoichiometric yield. At all temperatures, large chemical shifts were observed, with Curie and anti-Curie temperature dependencies indicative of strong hyperfine coupling between cysteine β-protons and mixed- or ferrous-valence iron, similar to those observed in natural protein environments(22) (Figure 2c,d, Figure S20). Combining the HYSCORE-based analysis, the computational ambidoxin model, and the temperature dependencies of NMR derived chemical shifts, we assigned three contact-shifted ^{1}H resonances to D-Cys2 and L-Cys5 H^β atoms, ligating a mixed-valence $Fe^{2.5+}$ pair, and two other ^{1}H resonances (Figure 2c) to D-Cys8 and L-Cys11 H^β atoms, ligating a ferrous Fe^{2+} pair (Figures S19 and S20). The temperature-dependent shifts were fully reversible and persistent at both pH 5 and pH 8.5 (Figure S20). These results demonstrate a stable peptide-cluster coordination structure around the bound paramagnetic 4Fe–4S center.

To test redox turnover stability, we performed cyclic voltammetry on a pyrolytic graphite edge electrode under anoxic conditions.(23) The midpoint potential of 4Fe–4S bound to **K** and **R** peptides at pH 8.5 (Figure 3a) was approximately –450 mV, which is within the range for extant bacterial ferredoxins.(24) One would expect the extensive hydrogen bonding and solvent exposure to reduce the Fe–S bond covalency and produce a species with a less reductive potential than bacterial ferredoxin,(25) but electrostatic contributions from **K** and **R** ambidoxin side chains appear to compensate, leading to a more reductive midpoint potential. Measurement of peak currents at different scan rates confirmed that current was not diffusion limited, and was due to direct electron transfer between the working electrode a metallo-peptide film(26) (Figure 3b). The holo-peptide endures hundreds of redox turnovers at room temperature, decaying with a rate constant of around 0.2% per cycle (Figure 3c). This robust redox stability exceeds that of many previously designed artificial metallo-peptides by ten to a hundred-fold. As in natural iron–sulfur proteins such as ferredoxin and rubredoxin, ambidoxin redox stability likely originates from the extensive network of second-shell hydrogen bonds from backbone amides to cysteine thiols and cluster μ-sulfurs.(27,28)

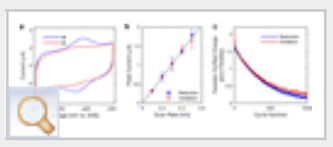

Figure 3. Electrochemical characterization of ambidoxin. (a) Cyclic voltammogram of **R** peptide (blue trace) and **K** peptide (red trace) at room temperature, pH 8.5. (b) Peak faradaic current of **R** peptide measured at different scan rates. (c) Measured faradaic charge from oxidation (red) and reduction (blue) of **R** peptide repeated over 1000 reduction–oxidation cycles. The rate decay constant estimated from exponential fits (dotted lines) is approximately 0.002 per cycle.

On the basis of analysis of a protein sequence in 1966, Eck and Dayhoff proposed that the ancestral ferredoxin might have had a repeating four-amino-acid pattern.(29) Since then, there have been many attempts to make minimal ferredoxin-like peptides based on similar sequence repeats.(30–33) The ambidoxin design, based on repeating structural features rather than

sequence, produced a simple, artificial ferredoxin that closely mimics redox behavior of its biologically evolved counterparts. Such structural and sequence simplicity greatly increases the likelihood of prebiotic evolution of catalytic redox-active peptides on early Earth.(34) Molecules much like the ambidoxins may have served as soluble electron carriers prior to the emergence of homochirality required for protein translation and folding.(35) In this scenario, ambidoxin would have assembled from racemic sources of amino acids present in the environment, with peptide bonds formed abiologically, near hydrothermal vents(36) or on mineral surfaces.(37)

Wächtershäuser and others proposed short heterochiral peptides with catalytic metal centers were critical intermediates in the earliest stages of chemolithotrophic origins of life.(38,39) The robust redox stability of ambidoxins is a clear demonstration in the laboratory that early peptide catalysts could have been functionally on par or even superior to modern proteins in some respects. Without chaperones, metal cluster biogenesis and homeostasis mechanisms present in a cellular milieu, early peptides had to specifically and stably coordinate metals in order to be effective catalysts.(40) This is in contrast to the view of early enzymes as poorly functioning ancestors of modern catalysts.(41,42) Geometric calculations indicate multiple solutions for short heterochiral molecules that form rings of different lengths (Supporting Information). Ambidoxins may be just one case in a larger family of metal-chelating peptides that could have served as prebiotic molecular ancestors for redox catalysts that sparked the emergence of modern oxidoreductases.

Supporting Information

Jump to a section

The Supporting Information is available free of charge on the ACS Publications website at DOI: 10.1021/jacs.8b07553.

- Experimental details (PDF)

PDF

- ja8b07553_si_001.pdf (4.33 MB)

Minimal Heterochiral *de Novo* Designed 4Fe–4S Binding Peptide Capable of Robust Electron Transfer

+Author Present Address
Physiological Communications Research Group, Nokia Bell Laboratories, 600 Mountain Avenue, Murray Hill, NJ 07974

¶Author Contributions
These authors contributed equally.

The authors declare the following competing financial interest(s): J.D.K., D.H.P, V.N. and P.G.F. are inventors on a patent application submitted by Rutgers, the State University of New Jersey. G.T.M. is founder of Nexomics Bioscience, Inc.

Acknowledgments

Jump to a section

We thank Drs. Andrew Mutter, Antonio Rosato and Lucia Banci for helpful discussions and Dr. Kevin Wyman for technical assistance. This work was supported by a grant from the Gordon and Betty Moore Foundation on “Design and Construction of Life’s Transistors” (GBMF-4742) to V.N. and P.G.F. and by NIH shared instrumentation grant (1S10OD018207-01) to G.T.M.

References

Reference QuickView
Jump to a section

This article references 42 other publications.

1. Johnson, D. C.; Dean, D. R.; Smith, A. D.; Johnson, M. K. Structure, function, and formation of biological iron-sulfur clusters. *Annu. Rev. Biochem.* **2005**, *74*, 247– 281, DOI: 10.1146/annurev.biochem.74.082803.133518 [Crossref], [PubMed], [CAS] Get it @ R
2. Raanan, H.; Pike, D. H.; Moore, E. K.; Falkowski, P. G.; Nanda, V. Modular origins of biological electron transfer chains. *Proc. Natl. Acad. Sci. U. S. A.* **2018**, *115* (6), 1280– 1285, DOI: 10.1073/pnas.1714225115 [Free @ PNAS], [Crossref], [PubMed], [CAS] Get it @ R
3. Chandonia, J.-M.; Fox, N. K.; Brenner, S. E. SCOPe: Manual Curation and Artifact Removal in the Structural Classification of Proteins – extended Database. *J. Mol. Biol.* **2017**, *429* (3), 348– 355, DOI: 10.1016/j.jmb.2016.11.023 [Crossref], [PubMed], [CAS] Get it @ R
4. Adman, E. T.; Sieker, L. C.; Jensen, L. H. The structure of a bacterial ferredoxin. *J. Biol. Chem.* **1973**, *248* (11), 3987– 3996 [PubMed], [CAS] Get it @ R
5. Orengo, C. A.; Thornton, J. M. Protein families and their evolution-a structural perspective. *Annu. Rev. Biochem.* **2005**, *74*, 867– 900, DOI: 10.1146/annurev.biochem.74.082803.133029 [Crossref], [PubMed], [CAS] Get it @ R
6. Kim, J. D.; Rodriguez-Granillo, A.; Case, D. A.; Nanda, V.; Falkowski, P. G. Energetic selection of topology in ferredoxins. *PLoS Comput. Biol.* **2012**, *8* (4), e1002463, DOI: 10.1371/journal.pcbi.1002463 [Crossref], [PubMed], [CAS] Get it @ R
7. Nanda, V.; Senn, S.; Pike, D. H.; Rodriguez-Granillo, A.; Hansen, W. A.; Khare, S. D.; Noy, D. Structural principles for computational and de novo design of 4Fe–4S metalloproteins. *Biochim. Biophys. Acta, Bioenerg.* **2016**, *1857* (5), 531– 538, DOI: 10.1016/j.bbabio.2015.10.001 [Crossref], [PubMed], [CAS] Get it @ R
8. Grzyb, J.; Xu, F.; Weiner, L.; Reijerse, E. J.; Lubitz, W.; Nanda, V.; Noy, D. De novo design of a non-natural fold for an iron–sulfur protein: Alpha-helical coiled-coil with a four-iron four-sulfur cluster binding site in its central core. *Biochim. Biophys. Acta, Bioenerg.* **2010**, *1797* (3), 406– 413, DOI: 10.1016/j.bbabio.2009.12.012 [Crossref], [PubMed], [CAS] Get it @ R
9. Roy, A.; Sarrou, I.; Vaughn, M. D.; Astashkin, A. V.; Ghirlanda, G. De novo design of an artificial bis [4Fe-4S] binding protein. *Biochemistry* **2013**, *52* (43), 7586– 7594, DOI: 10.1021/bi401199s [ACS Full Text], [CAS] Get it @ R
10. Pauling, L.; Corey, R. B. The Pleated Sheet, A New Layer Configuration of Polypeptide Chains. *Proc. Natl. Acad. Sci. U. S. A.* **1951**, *37* (5), 251– 256, DOI: 10.1073/pnas.37.5.251 [Free @ PNAS], [Crossref], [PubMed], [CAS] Get it @ R
11. Watson, J. D.; Milner-White, E. J.; Thornton, J. The conformations of polypeptide chains where the main-chain parts of successive residues are enantiomeric. Their occurrence in cation and anion-binding regions of proteins.. *J. Mol. Biol.* **2002**, *315* (2), 183– 191, DOI: 10.1006/jmbi.2001.5228 [Crossref], [PubMed],

[CAS] Get it @ R

12. Watson, J. D.; Milner-White, E. J. A novel main-chain anion-binding site in proteins: The nest. A particular combination of ϕ, ψ values in successive residues gives rise to anion-binding sites that occur commonly and are found often at functionally important regions. *J. Mol. Biol.* **2002**, *315* (2), 171– 182, DOI: 10.1006/jmbi.2001.5227 [Crossref], [PubMed], [CAS] Get it @ R

13. Rao, P. V.; Holm, R. H. Synthetic analogues of the active sites of iron-sulfur proteins. *Chem. Rev.* **2004**, *104* (2), 527– 560, DOI: 10.1021/cr020615+ [ACS Full Text], [CAS] Get it @ R

14. Bruice, T. C.; Maskiewicz, R.; Job, R. The Acid-Base Properties, Hydrolytic Mechanism, and Susceptibility to O(2) Oxidation of Fe(4)S(4)(SR)(4) Clusters. *Proc. Natl. Acad. Sci. U. S. A.* **1975**, *72* (1), 231– 4, DOI: 10.1073/pnas.72.1.231 [Free @ PNAS], [Crossref], [PubMed], [CAS] Get it @ R

15. Tagawa, K.; Arnon, D. I. Ferredoxins as Electron Carriers in Photosynthesis and in the Biological Production and Consumption of Hydrogen Gas. *Nature* **1962**, *195*, 537, DOI: 10.1038/195537a0 [Crossref], [PubMed], [CAS] Get it @ R

16. Bertrand, P.; Gayda, J. P.; Rao, K. K. Electron spin-lattice relaxation of the [4Fe-4S] ferredoxin from B. stearothermophilus - comparison with other iron proteins. *J. Chem. Phys.* **1982**, *76* (10), 4715– 4719, DOI: 10.1063/1.442788 [Crossref], [CAS] Get it @ R

17. Guigliarelli, B.; Bertrand, P. Application of EPR spectroscopy to the structural and functional study of iron-sulfur proteins. *Adv. Inorg. Chem.* **1999**, *47*, 421– 497, DOI: 10.1016/S0898-8838(08)60084-7 [Crossref], [CAS] Get it @ R

18. Ohnishi, T.; Ragan, C. I.; Hatefi, Y. EPR studies of iron-sulfur clusters in isolated subunits and subfractions of NADH-ubiquinone oxidoreductase. *J. Biol. Chem.* **1985**, *260* (5), 2782– 2788 [PubMed], [CAS] Get it @ R

19. Hofer, P.; Grupp, A.; Nebenfuhr, H.; Mehring, M. Hyperfine sublevel correlation (HYSCORE) spectroscopy - a 2D electron-spin-resonance investigation of the squaric acid radical. *Chem. Phys. Lett.* **1986**, *132* (3), 279– 282, DOI: 10.1016/0009-2614(86)80124-5 [Crossref] Get it @ R

20. Reijerse, E. J.; Dikanov, S. A. Electron-spin echo envelope modulation spectroscopy on orientationally disordered systems: Line-shape singularities in S = 1/2, I = 1/2 spin systems. *J. Chem. Phys.* **1991**, *95* (2), 836– 845, DOI: 10.1063/1.461091 [Crossref], [CAS] Get it @ R

21. Brancaccio, D.; Gallo, A.; Mikolajczyk, M.; Zovo, K.; Palumaa, P.; Novellino, E.; Piccioli, M.; Ciofi-Baffoni, S.; Banci, L. Formation of [4Fe-4S] Clusters in the Mitochondrial Iron–Sulfur Cluster Assembly Machinery. *J. Am. Chem. Soc.* **2014**, *136* (46), 16240– 16250, DOI: 10.1021/ja507822j ACS Full Text, [CAS] Get it @ R

22. Antonkine, M. L.; Bentrop, D.; Bertini, I.; Luchinat, C.; Shen, G.; Bryant, D. A.; Stehlik, D.; Golbeck, J. H. Paramagnetic 1H NMR spectroscopy of the reduced, unbound Photosystem I subunit PsaC: sequence-specific assignment of contact-shifted resonances and identification of mixed-and equal-valence Fe-Fe pairs in [4Fe-4S] centers FA- and FB-. *JBIC, J. Biol. Inorg. Chem.* **2000**, *5* (3), 381– 392, DOI: 10.1007/PL00010667 [Crossref], [PubMed], [CAS] Get it @ R

23. Armstrong, F. A.; Heering, H. A.; Hirst, J. Reaction of complex metalloproteins studied by protein-film voltammetry. *Chem. Soc. Rev.* **1997**, *26* (3), 169– 179, DOI: 10.1039/cs9972600169 [Crossref], [CAS] Get it @ R

24. Liu, J.; Chakraborty, S.; Hosseinzadeh, P.; Yu, Y.; Tian, S.; Petrik, I.; Bhagi, A.; Lu, Y. Metalloproteins containing cytochrome, iron–sulfur, or copper redox centers. *Chem. Rev.* **2014**, *114* (8), 4366– 4469, DOI: 10.1021/cr400479b [ACS Full Text], [CAS] Get it @ R

25. Dey, A.; Jenney, F. E.; Adams, M. W.; Babini, E.; Takahashi, Y.; Fukuyama, K.; Hodgson, K. O.; Hedman, B.; Solomon, E. I. Solvent tuning of electrochemical potentials in the active sites of HiPIP versus ferredoxin. *Science* **2007**, *318* (5855), 1464– 1468, DOI: 10.1126/science.1147753 [Crossref], [PubMed], [CAS] Get it @ R

26. Léger, C.; Elliott, S. J.; Hoke, K. R.; Jeuken, L. J.; Jones, A. K.; Armstrong, F. A. Enzyme electrokinetics: using protein film voltammetry to investigate redox enzymes and their mechanisms. *Biochemistry* **2003**, *42* (29), 8653– 8662, DOI: 10.1021/bi034789c [ACS Full Text], [CAS] Get it @ R

27. Blake, P. R.; Park, J. B.; Adams, M. W. W.; Summers, M. F. Novel observation of NH--S(Cys) hydrogen-bond-mediated scalar coupling in cadmium-113 substituted rubredoxin from Pyrococcus furiosus. *J. Am.*

Chem. Soc. **1992**, *114* (12), 4931– 4933, DOI: 10.1021/ja00038a084 ACS Full Text, [CAS] Get it @ R

28. Backes, G.; Mino, Y.; Loehr, T. M.; Meyer, T. E.; Cusanovich, M. A.; Sweeney, W. V.; Adman, E. T.; Sanders-Loehr, J. The environment of Fe4S4 clusters in ferredoxins and high-potential iron proteins. New information from x-ray crystallography and resonance Raman spectroscopy. *J. Am. Chem. Soc.* **1991**, *113* (6), 2055– 2064, DOI: 10.1021/ja00006a027 ACS Full Text, [CAS] Get it @ R

29. Eck, R. V.; Dayhoff, M. O. Evolution of the structure of ferredoxin based on living relics of primitive amino acid sequences. *Science* **1966**, *152* (3720), 363– 366, DOI: 10.1126/science.152.3720.363 [Crossref], [PubMed], [CAS] Get it @ R

30. Gibney, B. R.; Mulholland, S. E.; Rabanal, F.; Dutton, P. L. *Proc. Natl. Acad. Sci. U. S. A.* **1996**, *93* (26), 15041– 15046, DOI: 10.1073/pnas.93.26.15041 [Free @ PNAS], [Crossref], [PubMed], [CAS] Get it @ R

31. Nanda, V.; Rosenblatt, M. M.; Osyczka, A.; Kono, H.; Getahun, Z.; Dutton, P. L.; Saven, J. G.; DeGrado, W. F. De Novo Design of a Redox-Active Minimal Rubredoxin Mimic. *J. Am. Chem. Soc.* **2005**, *127* (16), 5804– 5805, DOI: 10.1021/ja050553f ACS Full Text, [CAS] Get it @ R

32. Benson, D. E.; Wisz, M. S.; Hellinga, H. W. Rational design of nascent metalloenzymes. *Proc. Natl. Acad. Sci. U. S. A.* **2000**, *97* (12), 6292– 6297, DOI: 10.1073/pnas.97.12.6292 [Free @ PNAS], [Crossref], [PubMed], [CAS] Get it @ R

33. Grzyb, J.; Xu, F.; Nanda, V.; Łuczkowska, R.; Reijerse, E.; Lubitz, W.; Noy, D. Empirical and computational design of iron-sulfur cluster proteins. *Biochim. Biophys. Acta, Bioenerg.* **2012**, *1817* (8), 1256– 1262, DOI: 10.1016/j.bbabio.2012.02.001 [Crossref], [PubMed], [CAS] Get it @ R

34. Jelen, B. I.; Giovannelli, D.; Falkowski, P. G. The Role of Microbial Electron Transfer in the Coevolution of the Biosphere and Geosphere. *Annu. Rev. Microbiol.* **2016**, *70* (1), 45– 62, DOI: 10.1146/annurev-micro-102215-095521 [Crossref], [PubMed], [CAS] Get it @ R

35. Nanda, V.; DeGrado, W. F. Simulated Evolution of Emergent Chiral Structures in Polyalanine. *J. Am. Chem. Soc.* **2004**, *126* (44), 14459– 14467, DOI: 10.1021/ja0461825 ACS Full Text, [CAS] Get it @ R

36. Cleaves, H. J.; Aubrey, A. D.; Bada, J. L. An Evaluation of the Critical Parameters for Abiotic Peptide Synthesis in Submarine Hydrothermal Systems. *Origins Life Evol. Biospheres* **2009**, *39* (2), 109– 126, DOI: 10.1007/s11084-008-9154-1 [Crossref], [PubMed], [CAS] Get it @ R

37. Ferris, J. P.; Hill, A. R., Jr; Liu, R.; Orgel, L. E. Synthesis of long prebiotic oligomers on mineral surfaces. *Nature* **1996**, *381*, 59, DOI: 10.1038/381059a0 [Crossref], [PubMed], [CAS] Get it @ R

38. Huber, C.; Wachtershauser, G. Peptides by activation of amino acids with CO on (Ni,Fe)S surfaces: implications for the origin of life. *Science* **1998**, *281* (5377), 670– 672, DOI: 10.1126/science.281.5377.670 [Crossref], [PubMed], [CAS] Get it @ R

39. Milner-White, E. J.; Russell, M. J. Predicting the conformations of peptides and proteins in early evolution. A review article submitted to Biology Direct. *Biol. Direct* **2008**, *3*, 3, DOI: 10.1186/1745-6150-3-3 [Crossref], [PubMed], [CAS] Get it @ R

40. Dupont, C. L.; Butcher, A.; Valas, R. E.; Bourne, P. E.; Caetano-Anollés, G. History of biological metal utilization inferred through phylogenomic analysis of protein structures. *Proc. Natl. Acad. Sci. U. S. A.* **2010**, *107* (23), 10567– 10572, DOI: 10.1073/pnas.0912491107 [Free @ PNAS], [Crossref], [PubMed], [CAS] Get it @ R

41. Johnsson, K.; Allemann, R. K.; Widmer, H.; Benner, S. A. *Nature* **1993**, *365*, 530– 532, DOI: 10.1038/365530a0 [Crossref], [PubMed], [CAS] Get it @ R

42. Jiang, L.; Althoff, E. A.; Clemente, F. R.; Doyle, L.; Röthlisberger, D.; Zanghellini, A.; Gallaher, J. L.; Betker, J. L.; Tanaka, F.; Barbas, C. F.; Hilvert, D.; Houk, K. N.; Stoddard, B. L.; Baker, D. De Novo Computational Design of Retro-Aldol Enzymes. *Science* **2008**, *319* (5868), 1387– 1391, DOI: 10.1126/science.1152692 [Crossref], [PubMed], [CAS] Get it @ R

Harnessing Structural Dynamics in a 2D Manganese–Benzoquinoid Framework To Dramatically Accelerate Metal Transport in Diffusion-Limited Metal Exchange Reactions
Journal of the American Chemical Society
Liu, Li, DeGayner, Winegar, Fang, and Harris
0 (0),
Abstract Full Text HTML PDF w/ Links Hi-Res PDF

Polar Solvent Induced Lattice Distortion of Cubic $CsPbI_3$ Nanocubes and Hierarchical Self-Assembly into Orthorhombic Single-Crystalline Nanowires
Journal of the American Chemical Society
Sun, Huang, Liu, Xu, Zhang, Jiang, Xue, Xu, Ma, Ding, Ge, Gu, Fang, Zhong, Hu, and Wan
0 (0),
Abstract Full Text HTML PDF w/ Links Hi-Res PDF

Catalytic Alkene Difunctionalization via Imidate Radicals
Journal of the American Chemical Society
Nakafuku, Fosu, and Nagib